

# First steps towards interlocking modular microfluidic cooling substrates (i-M $\mu$ CS) for future silicon tracking detectors in High Energy Physics (HEP)

Massimo Angeletti<sup>a,b,\*</sup>, Philippe Renaud<sup>b</sup>, Corrado Gargiulo<sup>a</sup>

<sup>a</sup> Experimental Physics Department, European Laboratory for Particle Physics (CERN), Geneva 1211, Switzerland

<sup>b</sup> Microsystems Laboratory LMIS4, École Polytechnique Fédérale de Lausanne (EPFL), Lausanne 1015, Switzerland

## ARTICLE INFO

### Keywords:

Microfluidics  
Microchannels  
Fluidic interconnection  
Particle detectors  
Microchannel cooling substrate  
Additive manufacturing

## ABSTRACT

In future High Energy Physics detectors, the coverage of large surfaces with silicon pixel chip sensors poses a challenge for the sensors positioning, for their cooling, assembly, and interconnection. The use of a cooling substrate on which the sensors are glued is typically limited by the bulky and complicated hydraulic interconnection between adjacent substrates. In this research, a new type of cooling substrate is presented. Its design is based on microchannels, where additive manufacturing of plastic and ceramic materials has been considered an alternative to the current silicon etching process. A solution to the mechanical and hydraulic interconnection problem is achieved through a modular interlocking concept. Design optimisation was followed having identified three relevant parameters, plug-and-ply, interchangeability and sealing performance, which qualify the substrates interconnection and guaranty their correct positioning. This paper poses the bases to a new substrate category where modularity, re-workability and easy connectivity are the strong points. This concept could find applications also outside High Energy Physics experiments such as hardware cloud computing and medical detectors.

## 1. Introduction

The purpose of this research is to investigate a new modular cooling substrate for High Energy Physics (HEP) silicon detector and qualify its mechanical and hydraulic interconnection. The article is divided into four parts. The first paragraph, the introduction, presents an overview of the thermal management of silicon trackers used in HEP experiments. It explains the needs of implementing modular cooling substrate solutions for future detectors and introduces the new interconnection concept together with the materials and the additive manufacturing process identified for the investigation.

The second paragraph presents the experimental methodology to qualify the mechanical and hydraulic interconnection, considered as the key design feature for the modular concept implementation. While test results, design criticalities and optimizations are illustrated in paragraph three. Results summary and the next steps of the research are outlined in the conclusion paragraph.

### 1.1. Thermal management of silicon tracking detector

A silicon tracking detector reveals the paths of electrically charged

particles as they pass through and interact with the silicon chip sensors. These sensors are made by doping thin Silicon layers and transforming them into reverse-biased semiconductor p-n type diodes. In HEP experiments, silicon chip sensors are typically arranged into several coaxial cylindrical layers placed around the interaction point of the colliding beams [1].

Sensor thermal management and lightweight mechanics represent the major challenges, where the reduction of the material in the detection area is of particular importance for improving the overall detector resolution. Indeed, ultra-thin silicon sensors (~50–100  $\mu$ m thick) are kept in position and cooled by minimum-material (low-mass) “Substrates” [2]. The assembly of sensors and Substrate will be referred to, hereafter, as “Module”.

In the framework of the recent upgrade programs (2019–2021) for the Large Hadron Collider (LHC) at CERN, two main categories of low-mass cooling substrates emerged (Fig. 1), the “Carbon-Vascular Cooling Substrate” (CVCS) and the “Silicon Microchannel Cooling Substrate” (Silicon  $\mu$ CS). While the first allows the glueing of several sensors (up to 100) on a single Substrate, the second one permits few sensors’ cooling. The drawback of the first solution is the impossibility to rework or replace a single sensor. In contrast, the second approach is challenged by

\* Corresponding author at: CERN European Laboratory for Particle Physics, Geneva CH-1211, Switzerland.

E-mail addresses: [massimo.angeletti@cern.ch](mailto:massimo.angeletti@cern.ch) (M. Angeletti), [philippe.renaud@epfl.ch](mailto:philippe.renaud@epfl.ch) (P. Renaud), [corrado.gargiulo@cern.ch](mailto:corrado.gargiulo@cern.ch) (C. Gargiulo).

<https://doi.org/10.1016/j.mee.2022.111707>

Received 14 December 2021; Accepted 2 January 2022

Available online 7 January 2022

0167-9317/© 2022 The Authors. Published by Elsevier B.V. This is an open access article under the CC BY license (<http://creativecommons.org/licenses/by/4.0/>).

connectivity complexity among Substrates, required to cover a large detection area.

Future Si trackers for HEP experiments in hadron particle accelerators will have to operate in a high radiation level environment, up to 254 MGy for about 10 years, and the detection area of a Si tracker outermost layer will be around  $50 \text{ m}^2$  [6]. High radiation level will require efficient active cooling to extend the sensor's lifetime. The large surface coverage will call for the use of a modular concept, where Modules are mechanically and hydraulically interconnected, allowing easy testing and assembling while keeping the possibility to rework and replace faulty sensors. While in tracking detectors for future lepton colliders [7], the radiation environment will be less a concern and sensors cooling can be at ambient temperature, relaxing the Substrate design requirements, mainly driven by sensors positioning accuracy and re-workability.

### 1.2. Interlocking modular microfluidic cooling substrate

The mechanical and hydraulic interconnection between modules represents the key design features of the new substrate category named “interlocking Modular microfluidic Cooling Substrate” (i-M $\mu$ CS).

Some efforts have been made to define guidelines for microfluidics interconnection. However, standards are not available. The wide variety of solutions developed is mostly application oriented. Modular concepts are already implemented for Lab-on-a-chip (LOC) devices [8–12]. In this case, the mass flow rate and pressure range are less demanding than typical HEP cooling configurations. Microfluidic Substrates for cooling applications, found in literature, are typically limited to single chip cooling. Interconnections between Substrates have never been implemented in a real application. Nevertheless, some studies have been performed [13,14] also at CERN [15].

The design of the Substrate and its interconnection is driven by the coolant choice. In this paper, the fluid considered as the baseline is demineralised water at ambient temperature; nevertheless, the design targets the use of different coolants whose compatibility and thermal performance will be studied in a further step of the research.

The interconnection concept proposed in this paper is shown in the schematic in Fig. 2. Modules positioning and mechanical clamping is realized through a “Baseplate” whose pins engage the slots located at the back of the Substrate. Interference between pins and slots guarantees the Substrate's correct positioning and clamping.

An in-plane hydraulic interconnection is realized through a gasket pressed between the Substrates. The compression force of the gasket is provided by the pins and slots anchoring. The design challenge comes from the micro-dimensions of the features in the Substrate and in the Baseplate, affected by the accuracy that can be achieved in the

production.

As a preliminary proof of concept, it was decided to produce a prototype (Fig. 3), taking inspiration from commercial LEGO and preserving similar standard LEGO® dimensions, as in part was done by C. Owens [12]. Nevertheless, the geometry of the pin and slot, as well their interface, differs from standard LEGO® design, based on the necessity to include microchannels in the module and to minimize its thickness. No leaks up to 1 MPa have been detected in the experimental tests.

This proof of concept and the next steps towards dimension scaling to microfeatures are based on the additive manufacturing (AM) production process. The materials considered for the final Substrate are engineered polymers and ceramics, while this publication focuses on polymer only.

The choice of producing, as a first approach, Substrates in polymeric materials is based on the relative facility of 3D printing parts with micro features and the possibility to optimise their geometries rapidly. Nevertheless, even if the final target is to use ceramic, the polymeric Substrate can find applications in HEP trackers for lepton colliders where sensors can be operated at ambient temperature. Indeed, limiting factors of polymers are the low thermal conductivity and the mismatching of the coefficient of thermal expansion (CTE) with the silicon sensors (3–5 ppm/K). Taking as an example the 3D printable epoxy-based resin ACCURA25 [16], commonly used in HEP experiment for its radiation tolerance, its thermal conductivity and CTE are respectively  $0.150 \text{ W/m}^\circ\text{K}$  and  $107 \text{ ppm/K}$ .

However, minimization of the substrate thickness at the interface between coolant and sensor can reduce the impact of the polymer low thermal conductivity. Wall thickness of  $0.4 \text{ mm}$  has been demonstrated to be printable while still guaranteeing leak tightness of the cooling channels. Further thickness reduction is under study.

As an example, the ALPIDE Monolithic Active Pixel Sensor [17], used in ALICE, and dissipating about  $40 \text{ mW/cm}^2$ , can be kept at an operative ambient temperature by a polymeric substrate with chilled water at  $20^\circ\text{C}$  as coolant, Fig. 4. Ambient operative temperature also minimizes the effect of the CTE mismatching between silicon sensor and polymeric substrates with no relevant impact on sensor stability and integrity.

Finally, ceramic Substrates will suit HEP applications, like hadron collider trackers, where higher thermal performances and lower operative temperature ( $< -30^\circ\text{C}$ ) are required.

## 2. Method

The modular interconnection of the i-M $\mu$ CS should guaranty stable mechanical connection within the elastic regime of the different components, do not influence the precise Module positioning and satisfy the cooling requirement in terms of hydraulic pressure resistance.

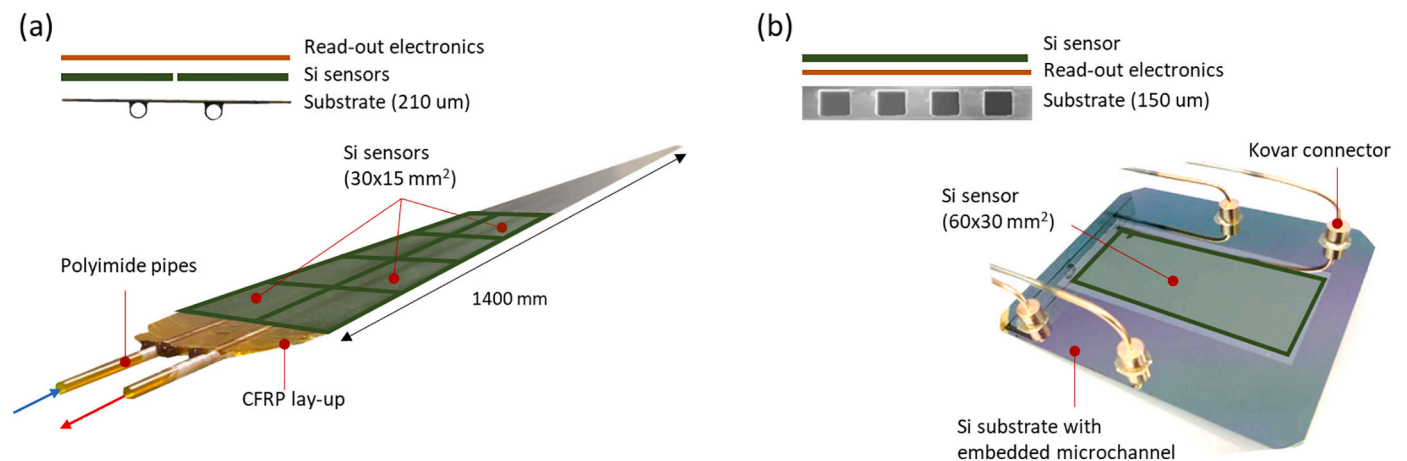


**Fig. 1.** Example of HEP low-mass cooling substrates: (a) CVCS solution of ALICE Inner Tracking System 2 (ITS2) detector [3] and (b) Si  $\mu$ CS solution chosen for NA62 Gigatracker (GTK) detector [4,5].

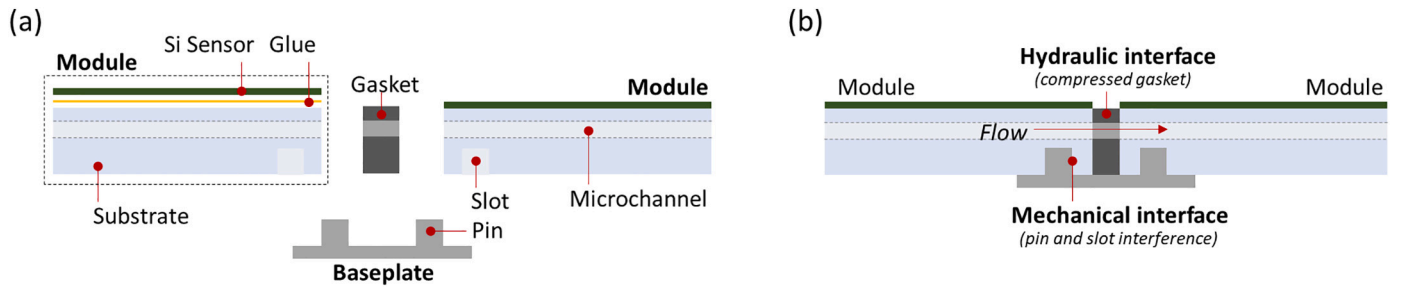


Fig. 2. Interlocking modular concept: Exploded view (a) and assembled view (b).

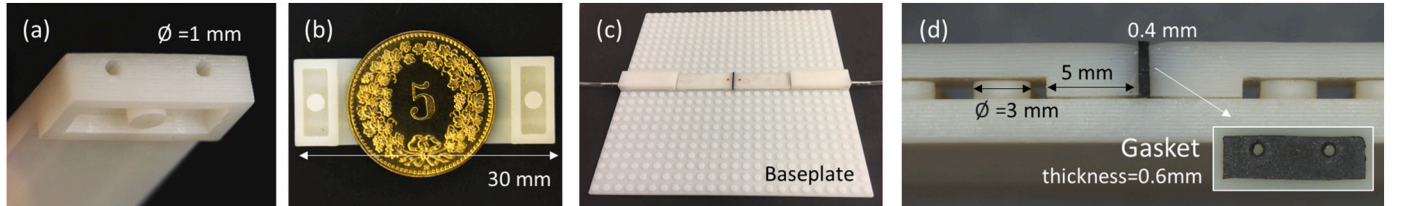


Fig. 3. Detail of the first prototype: Detail of the Substrate with two embedded channels (a), detail of the Substrate slot (b), Substrates and Baseplate assembly (c) and detail of the interconnection (d).

The experimental methodology to qualify the i-M $\mu$ CS interconnection followed an iterative process that involved analyses, prototypes production and tests. Different interconnection designs and polymer materials were investigated. Three relevant properties were identified to develop and validate the mechanical and hydraulic interconnection: Substrate plug-and-play, interchangeability and sealing performance. The key parameters affecting these three properties are the Substrate and Baseplate's dimensional accuracies.

The plug-and-play property can be represented by the pull force needed to mount and dismount a Substrate from the Baseplate. The force should avoid the sensor's damage during assembly while keeping in place the sensor stably. This force is determined by the static friction coefficient between pin and slot and depends on the materials of the Baseplate and Substrate. Therefore, the optimisation of the plug-and-play parameter in this phase of the design was not driven by the necessity to reach a specific range of pull-force, but instead, by the design of a mechanical interface that can be tuned according to the requirements of the specific chosen materials.

The interchangeability is the ability to select components at random and fit them together within proper positioning tolerances, typically of the order of  $50 \text{ }\mu\text{m}$  for HEP tracker sensors [2], while fulfilling plug-and-play and sealing requirements.

The sealing performance is quantified through the pressure at which the leak appears at the interface between Modules and depends on the coolant and its operational range. The requirement of  $0.3 \text{ MPa}$  is set for demineralised water applications that operate in leak-less mode. It corresponds to the safety margin with respect to the nominal operating pressure range that goes from  $0.02 \text{ MPa}$  to  $0.08 \text{ MPa}$  [21]. However, the qualification to higher-pressure resistance will allow to consider the solution for applications that operate with more demanding coolants.

The development of the interconnection design is based on the optimisation of the three identified key properties and relays on tests of polymeric Substrates, while prioritising design solutions that can be shared with the ceramic option that is the final target of this development.

### 3. Interconnection design

#### 3.1. Design optimisation versus dimensional accuracy

Many variables influence the accuracy of 3D print parts, such as orientation during the printing process, printing layer's thickness and printing technology. However, we can assume that the minimum dimensional accuracy obtained for the polymer Substrates by commercial additive manufacturing is of the order of  $50 \text{ }\mu\text{m}$  corresponding to a total standard deviation ( $\sigma_{tot}$ ) of  $25 \text{ }\mu\text{m}$ . With the Substrate features' dimensions close to the achievable accuracy, the following criticalities have been identified:

- The maximum contact pressure ( $p_{max}$ ) between pin and slot could cause punctual plastic deformation. For a given manufacturing accuracy, a corresponding minimum pin diameter must ensure to be within elastic regime during all different assembly steps.
- The Substrate slots, and therefore the Substrate itself, absorb most of the deformation induced by the pin and slot interference. The Substrate deformation is seen by the silicon sensor glued on it. The design should then be optimised such to have most of the deformation, coming from the interference between pin and slot, absorbed by the pin instead.
- The Substrate accuracy has an impact on the dimension of the clearance between two adjacent Substrate surfaces where a sealed hydraulic interface is realized by a gasket, and this is reflected in a change of the pressure force compressing the gasket. Such force induces deformations that can compromise the alignment and, consequently, the sealing.
- The gasket dimension should be decreased down to the minimum admissible value, which guarantees the sealing, to minimize the required compressive force. Consequently, the contribution of the resultant force between the pins and the slots, due to the gasket compression force, is also minimized and it will facilitate the module mounting.

Based on the above considerations, a design for the Substrate and the Baseplate has been developed (Fig. 5). The pin diameter is set to  $3 \text{ mm}$  and sectioned in four quarters. This minimizes the contact pressure  $p_{max}$  while not compromising the single pin's pull force contribution. The

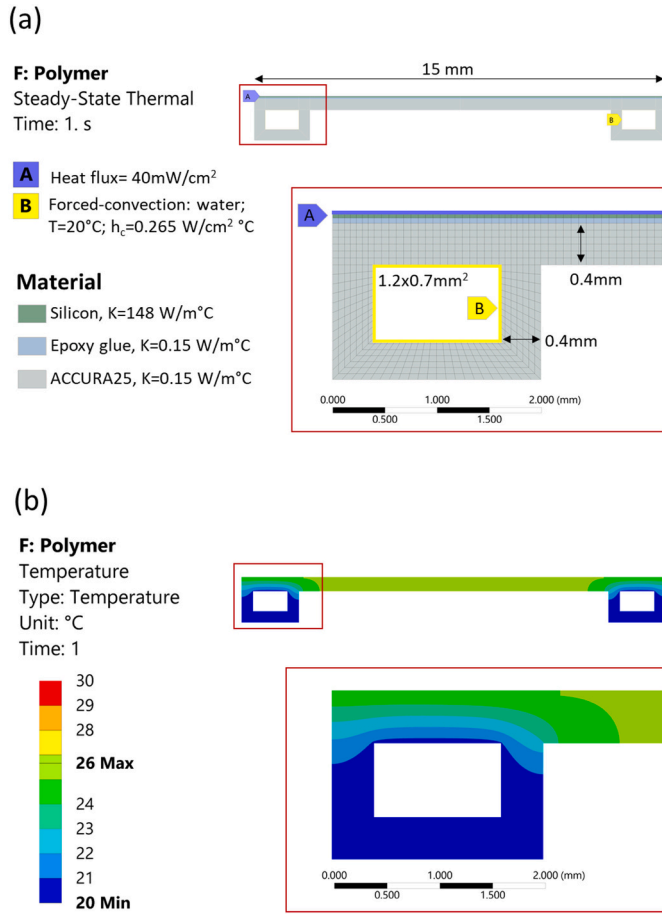


**Fig. 4. 2D thermal analysis of the ALPIDE sensor glued on a polymeric cooling Substrate:** Boundary conditions (a) and temperature results (b). The ALPIDE sensor is  $15 \times 30 \text{ mm}^2$  large and  $50 \mu\text{m}$  thin. Conservatively, an epoxy glue thickness of  $100 \mu\text{m}$  is considered at the interface between the sensor and Substrate. Two channels, with a rectangular cross-section of  $1.2 \times 0.7 \text{ mm}^2$ , are engraved in the polymers. The channels are perpendicular to the short side of the ALPIDE sensor corresponding to  $15 \text{ mm}$  length. The coolant is water at  $20^\circ\text{C}$  with a mass flow rate of  $0.1 \text{ g/s}$ . It operates in a laminar flow regime under the hypothesis of a constant axial wall heat flux. The corresponding Nusselt number is  $3.92$  and the convective heat transfer coefficient ( $h_c$ ) is  $0.265 \text{ W/cm}^2^\circ\text{C}$  [18,19]. The maximum temperature, reached in the sensor centre, is  $26^\circ\text{C}$ . The Ansys Workbench 2019 software [20] has been used to perform the analysis.

step between pins is  $5 \text{ mm}$ , and the dimension of the square slot is also set to  $3 \text{ mm}$  by design.

Sectioning in four quarters allows the pin to absorb most of the displacements coming from the interference between pin and slot, minimizing at the same time the deformation of the slots' wall in the Substrate. An additional feature was introduced to enhance the pin compliance by shaping the pin's basis with a fillet whose radius can be adjusted at the design level to tune the final pin stiffness (Fig. 5.b). The misalignment and possible uncoupling of the Substrates were minimized by optimising its relative position with respect to the channel interconnection (Fig. 5.c); the height in contact between pin and slot is  $1.5 \text{ mm}$ . The acceptable manufacturing tolerances can be larger because of the larger elastic deformation of the pin (Fig. 6).

Micro O-rings were considered for the hydraulic interconnection, minimizing the surface in contact and, therefore, the force required for the correct sealing compression. A groove with a depth of  $0.35 \text{ mm}$ , where the micro-O-ring sits (Fig. 5), was implemented in the design. The minimum elastomer thickness that guarantees the sealing, considering assembly tolerances, is  $0.45 \text{ mm}$ . The minimum O-ring's production

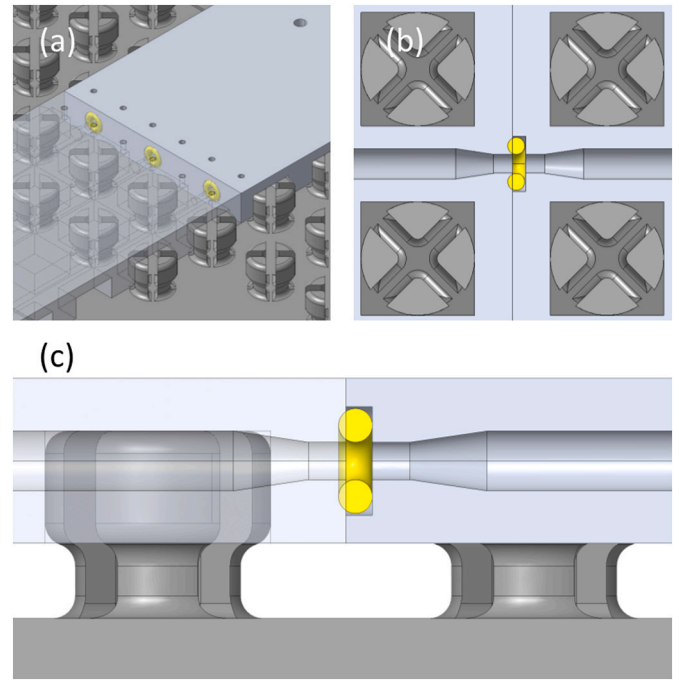


**Fig. 5. Design interconnection:** Isometric view (a), top section view (b) and lateral section view of the O-ring face seal (c).

tolerance is  $\pm 0.03 \text{ mm}$ .

When the O-ring is squeezed between the two surfaces forming a seal, an initial contact pressure appears between the O-ring and the surfaces. The seal is guaranteed as far as the fluid pressure is lower than the initial contact pressure. A further increase of fluid pressure induces the O-ring to be tighter compressed into the groove and, therefore, it leads to a further increase of the contact pressure. This circular relationship of increasing pressure leading to increased sealing is called “self-energizing” [22,23]. In our configuration, the O-ring fails when the clearance between the two adjacent surfaces increases due to the involved forces in the O-ring.

The breadboard model to qualify the interlocking modular micro-fluidic interconnection can be seen in Fig. 6.a. A specific AM material jetting technology, the “Stratasys Polyjet” [24], based on the use of sacrificial material inside the cooling channels, removed at the end of the process, was demonstrated to be the most promising process and affordable solution for prototyping. Straight and clear channels with inner diameters of  $1$ ,  $0.7$  and  $0.5 \text{ mm}$  were embedded in Substrates produced in Vero resin (acrylate photopolymer, [25]).

### 3.2. Validation and tests results

#### 3.2.1. Analysis of pin and slot interference

Based on the estimated values of position tolerance ( $\sigma_{pos}$ ) and dimensional tolerance ( $\sigma_{dim}$ ) for both Substrate and Baseplate, the pin coupling in the slot has an interference that goes from  $0$  to  $54 \mu\text{m}$ , assuming zero interference as a design specification (Fig. 7).

Finite element analysis (FEA) of the contact stress was performed to determine the effective interface behaviour (Fig. 8). As expected, the pin's elastic deformation absorbs the interference. There is no relevant deformation or stress in the slot, while the stress in the pin is well within the yield strength of Vero material ( $50\text{--}65 \text{ MPa}$  [25]). The maximum Von-mises stress is  $26 \text{ MPa}$  giving a yield safety factor of  $1.9$ . The perpendicular force acting into a pin quarter ( $F_{\perp}$ ) is of the order of  $0.45 \text{ N}$  and can be tuned by changing the pin's tapering.



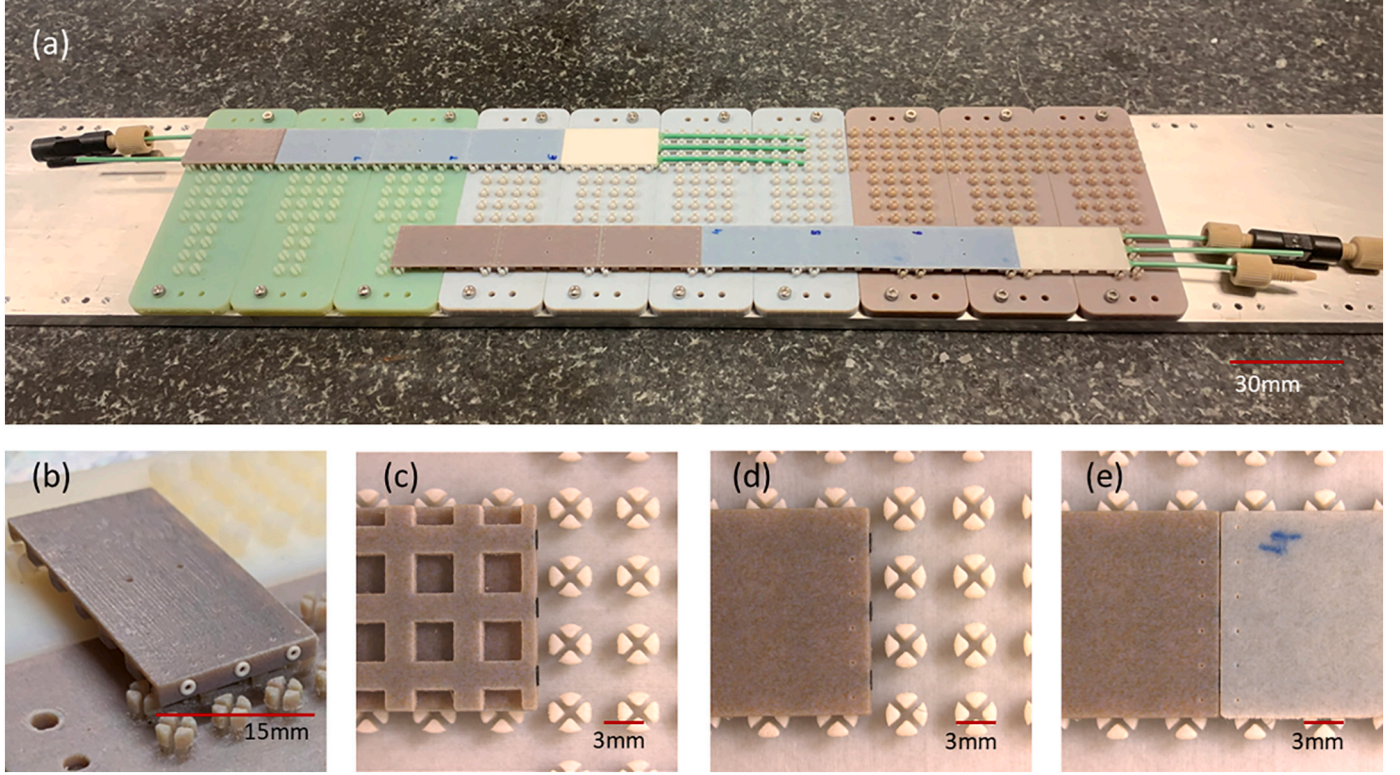


**Fig. 6. Breadboard model of the optimised interlocking configuration:** Assembly of Substrates and Baseplates (a), isometric view of the Substrate (b), detail of the Substrate slot (c) and top view of the interconnection assembly (d)(e). The Substrate used to test the interlocking interconnection is 30 mm × 15 mm large and 2.2 mm thick, while the Baseplate provides a different number of pins depending on the Substrate position.

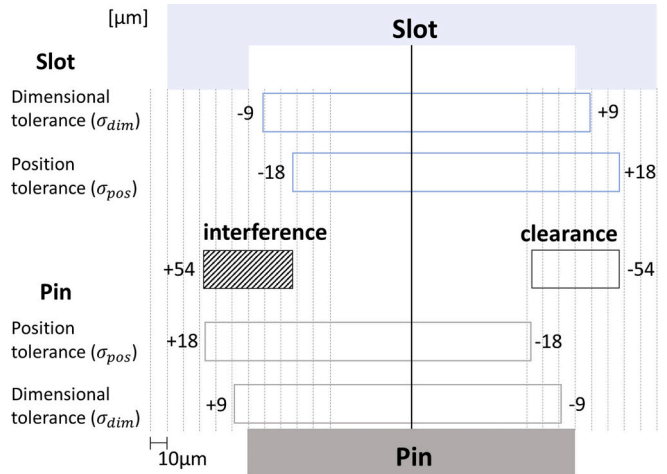


**Fig. 7. Pin-slot interference dependence on accuracy.** This schematic picture summarises the position and dimensional tolerances for pin and slot. The total tolerance ( $\sigma_{tot} = 25 \mu\text{m}$ ) is the sum in quadrature of position tolerance ( $\sigma_{pos}$ ) and dimensional tolerance ( $\sigma_{dim}$ ). Conservatively, we assumed  $\sigma_{tot}$  equally shared between  $\sigma_{pos}$  and  $\sigma_{dim}$ . This results in a value of  $18 \mu\text{m}$  for each term.

### 3.2.2. Substrate plug-and-play

The pull force needed to dismount a Substrate from the Baseplate was measured by a dynamometer attached to the Substrate (Fig. 9.a). Different Baseplate layouts that would provide different numbers of pins engaging the Substrate were considered. The number of pins engaging the Substrate and, therefore, the number of contact points (28, 56 or 84) depends on the number of rows of the breadboard model Baseplate (2, 4 or 6) on which the Substrate is mounted (Fig. 6a).

In Fig. 9.b, the average pull force value of each Substrate tested ranges between 1.5 N and 7 N depending on the number of contact points, and it linearly depends on them. The obtained pull force values point out that the specific design for the tested polymeric solution can provide a stable connection. At the same time, the Baseplate design features, like numbers of pins and pin geometry, guarantee that stable connections can also be achieved for different materials by simply tuning these features. The achieved flexibility of the pin design also minimizes the design dependence on the Modules' material choice, allowing to consider ceramic materials for the Substrate.

### 3.2.3. Substrate interchangeability

The Interchangeability ( $I_s$ ) is the ability to select components at random and fit them together within proper “Repeatability” ( $R_s$ ) and “Exchangeability” ( $E_s$ ). The accuracy of the Repeatability can be described as the accuracy in the position of the same Substrate once it is dismounted and mounted from the Baseplate. While, the accuracy of the Exchangeability is the accuracy in the position of different Substrates on the same Baseplate. Assuming the respective variances are independent and normally distributed,  $I_s$  can be defined as the sum in quadrature of  $R_s$  and  $E_s$  (Eqn 1).

$$I_s = \sqrt{R_s^2 + E_s^2} \quad (1)$$

The elastic averaging theory must be considered to investigate the Interchangeability property [26,27]. When several pins fit into several slots, the compliant pins deform slightly, causing an elastic averaging of the Substrate position and minimizing its total error.  $R_s$  and  $E_s$  are approximately inversely proportional to  $\sqrt{n}$  where  $n$  is the number of contact points.  $E_s$  also depends on the production process accuracy and precision as well as correlated to component orientation during printing. The Repeatability is considered accepted when it is negligible compared to  $E_s$  accuracy.

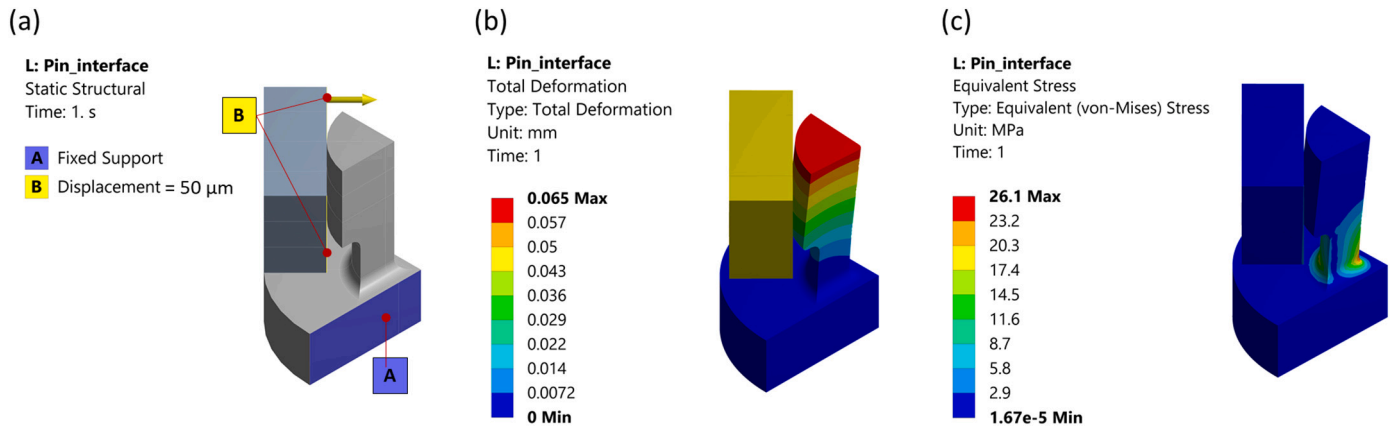


**Fig. 8. FEA Analysis of the pin-slot interface:** Boundary conditions (a), deformation of the pin and slot (b) and contact stress (c). Non-linear frictionless contact was conservatively assumed between pin and slot. The analysis was performed on a quarter of pin, and interference of 50  $\mu\text{m}$ , corresponding to a rounded value for the calculated maximum interference, was considered. The Ansys Workbench 2019 [20] software has been used to perform the analysis. The solution was obtained through iterative steps based on force convergence criteria.

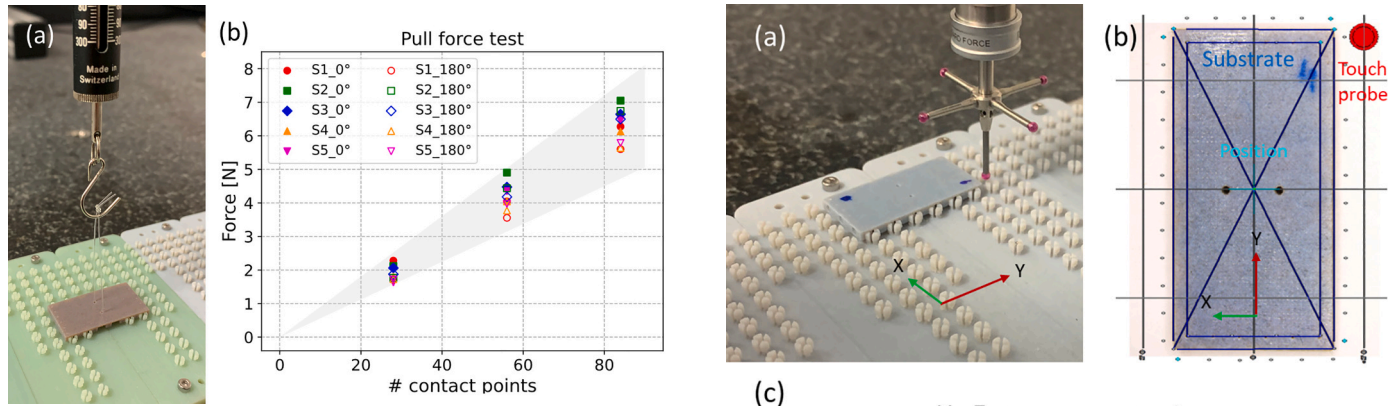


**Fig. 9. Pull force due to pin and slot interference.** Each sample (S1-S5) was tested eight times (a), and the orientation with respect to the Baseplate pins ( $0^\circ$  or  $180^\circ$ ) was inverted to verify the influence of pins position accuracy only. The plot shows the average pull force value of each sample for each contact points configuration (b).

Several measurements on the prototypes were performed for the experimental characterization of the Interchangeability. The measurements were carried out under a Coordinate Measuring Machine (CMM) by using a touch trigger probe as in Fig. 10.a.  $R_s$  was evaluated by mounting and dismounting the same Substrate ten times and calculating the standard deviation of the ten measurements (Fig. 11.b). While  $E_s$  was evaluated by calculating the standard deviation of the average position of the different Substrates mounted on the same Baseplate (Fig. 11.c).

The evaluated standard deviation of the Repeatability is approximately 1  $\mu\text{m}$  (Fig. 11.b) while the Interchangeability standard deviation goes from 10  $\mu\text{m}$  to 8  $\mu\text{m}$  depending on the number of contact points (Fig. 11.c). In our case, the Repeatability dependence on contact points is almost negligible. The study is limited by the number of the available samples and the number of performed measurements. However, the interlocking design has shown to provide alignment tolerances within 10  $\mu\text{m}$  even being the 3d printed parts within 25  $\mu\text{m}$  accuracy, thanks to the multi-pin elastic contacts. This has also positive implications in the hydraulic interconnection that relies on the compression of the sealing O-ring, dependent on the clearance between Modules.

### 3.2.4. Substrate sealing

The design of the hydraulic interface has been driven by the necessity to guarantee a minimum elastomer compression of 10% considering all

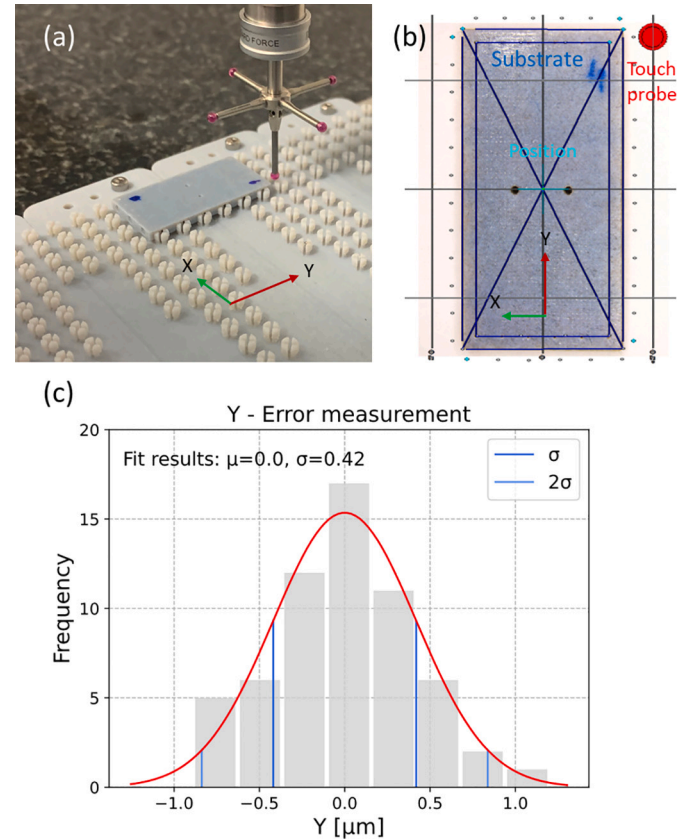


**Fig. 10. Measurement of the Substrate positioning.** A touch trigger probe (Renishaw TP200) integrated into the Mitutoyo CRISTA Apex S9206 CMM was used (a) [28]. The position of the Substrate centre was derived from the measurement of the Substrate edges (b). A study of the machine accuracy and precision was also performed. In this case, the position of a unmoved Substrate was measured, and the measurement repeated 60 times. The error measurement has a standard deviation less than 0.5  $\mu\text{m}$  (c).

the component tolerances [22], Table 1. The silicone O-ring, utilised for the test, has a cross-section (CS) diameter of 0.45 mm, an inner diameter (ID) of 0.5 mm and Shore A70. The depth of the Substrate groove is 0.35 mm and the nominal clearance between two adjacent Substrates is set to zero corresponding to a nominal gasket compression of 22%.

Tests to evaluate the pressure at which the hydraulic interface fails



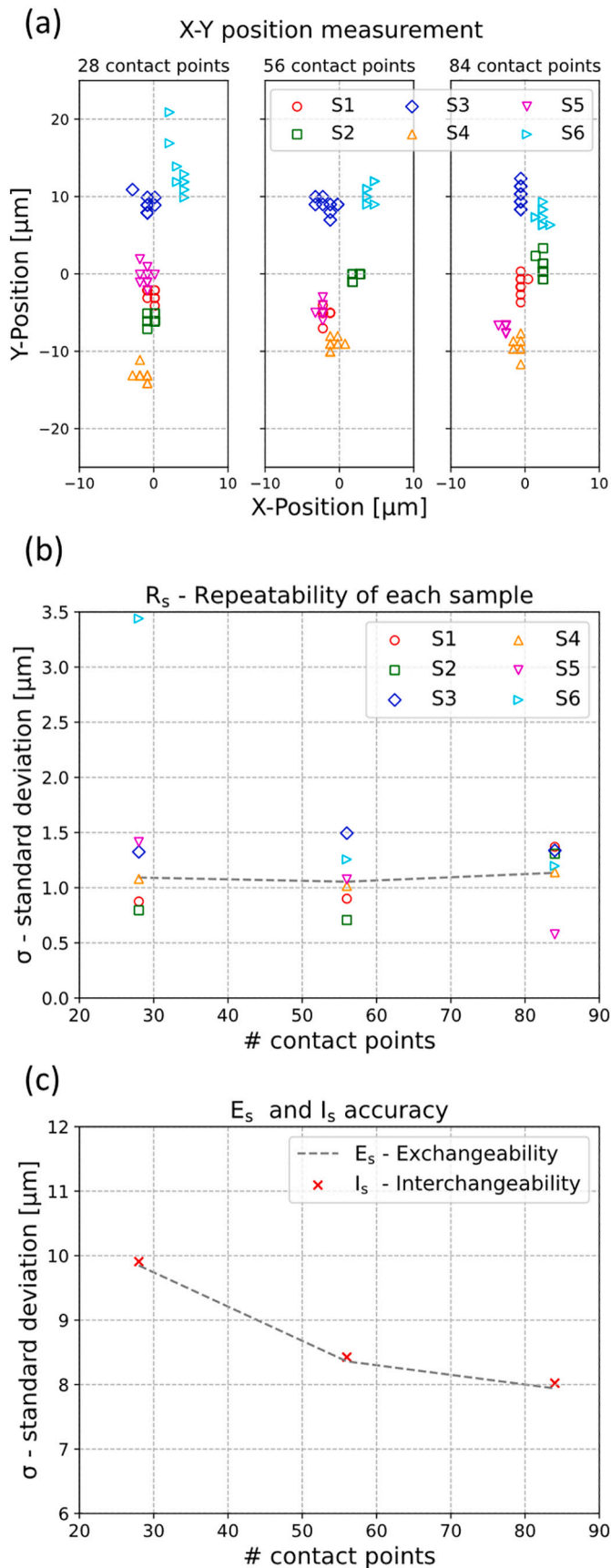


**Fig. 11. Repeatability and Interchangeability:** X and Y position measurements (a), Repeatability standard deviation of each Substrate and Repeatability mean value (b), Interchangeability and Exchangeability standard deviations (c).

**Table 1**

Design parameters of the hydraulic interface.

<b>Micro O-ring</b>	
Material	Silicone
Durometers [Shore A]	70
ID [mm]	0.5
CS diameter [mm]	0.45
Tolerance[mm]	$\pm 0.03$
<b>Groove</b>	
OD [mm]	1.4
Depth[mm]	0.35
Clearance[mm]	0
Tolerance[mm]	$\pm 0.025$
<b>Assembly</b>	
Tolerance	$\pm 0.025$
<b>Compression</b>	
Minimum	11%
Nominal	22%
Maximum	40%

were carried out. Substrates were mounted in series, up to 5 Substrates, and their order was modified for each trial (Fig. 12.a). Different numbers of contact points were considered. Fig. 12.b shows that the samples anchored to 84 contact points can reach pressure up to 4 MPa, before having a small leak at one of the hydraulic interfaces at the extremity of the Substrate chain. The leak pressure depends on the number of engaged pins (Fig. 12.c), and higher pressure can be reached by increasing the rigidity of the pins within elastic limits.

The sealing dependence on the coefficient of thermal expansion (CTE) is negligible when water is considered as coolant and ambient temperature as the operative one. Nevertheless, a minimum and maximum operative temperature range must be identified for a more general characterization of the Substrate, contextually with the Baseplate and Substrate materials choice.

Another aspect that should be considered is the long-term reliability as the interconnection should remain unchanged over time. Materials creep could affect long-term performance. Accelerating ageing test with thermal humidity and radiation environment can be done to assess the component's end-of-life properties.

#### 4. Conclusion

A completely new design for microchannel cooling substrates was developed based on an interlocking modular concept. Its production feasibility through additive manufacturing was demonstrated, polymers prototypes were produced and extensively tested. It was shown that i-MuCS can be easily assembled to cover large surface, overcoming the typical  $\mu\text{CS}$  interconnectivity problem, while keeping the possibility to rework and replace a single faulty Module.

Based on the first optimisation, several parameters, both for the mechanical and the hydraulic interface, were tuned to match specific design requirements. The Interchangeability, i.e., the ability to select modules at random and fit them together within proper tolerances, showed to guarantee the modules correct positioning and alignment within  $\pm 20 \mu\text{m}$ . The pull force needed to remove a Substrate from its Baseplate were measured in the range between 1.5 N and 7 N as proof of the stable module positioning, while allowing at the same time, a perfect mounting and dismounting capability. The hydraulic interconnected Substrates were tested up to 4 MPa without leaking.

The above conditions realized with polymeric Substrates match already HEP applications limited to ambient operative temperature, and the extension of these limits will be further investigated.

The interlocking modular microchannel design is being now optimised for additive manufacturing with ceramics material engineered for better thermoelastic compatibility with the silicon sensors used in HEP experiment and for operative temperature below  $0^\circ\text{C}$ .

The modular interlocking concept has also potentialities for applications outside HEP experiments, such as hardware cloud computing

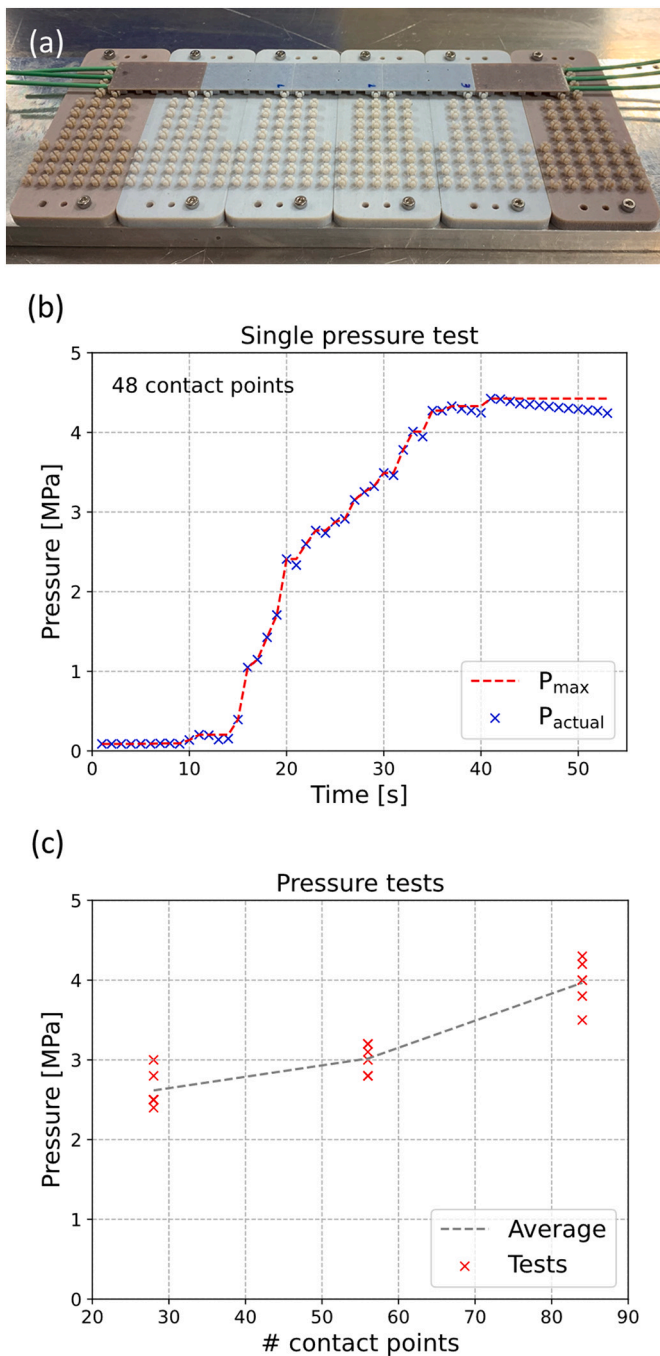


**Fig. 12. Pressure test results:** Samples in position (a), single pressure test (b), evaluation of the average pressure failure for different contact point configurations (c). The pressure sensor utilised is MEAS U5156-000005-100BA [29], and its pressure range goes from 0 to 10 MPa absolute with an accuracy of  $\pm 0.75\%$  full scale (FS) corresponding to an accuracy of  $\pm 0.075$  MPa.

and medical detectors. In the data centre field, minimizing the volume occupied by the cooling components and the possibility to replace hardware parts quickly will maximise the ratio between the total storage data memory and the total instrument occupancy volume. It could also reduce construction and maintenance costs.

#### Declaration of Competing Interest

None.

#### Acknowledgements

This work was supported by CERN Experimental Physics Department funding devoted to the research and development on technologies for future experiments.

#### References

- [1] F. Hartmann, *Evolution of Silicon Sensor Technology in Particle Physics* vol. 275, Springer International Publishing, Cham, 2017, pp. 1–133.
- [2] M. Aleksa, et al., Strategic R&D Programme on Technologies for Future Experiments [Online]. Available: <https://cds.cern.ch/record/2649646>, Dec. 2018.
- [3] M. Gomez Marzoo, *Innovative Low-Mass Cooling Systems for the ALICE ITS Upgrade Detector at CERN*, CERN-THESIS-2016-160 (2016) 99–146.
- [4] A. Mapelli, et al., Low material budget microfabricated cooling devices for particle detectors and front-end electronics, *Nucl. Phys. B - Proc. Suppl.* 215 (1) (Jun. 2011) 349–352, <https://doi.org/10.1016/j.nuclphysbps.2011.04.050>.
- [5] G. Romagnoli, et al., Silicon micro-fluidic cooling for NA62 GTK pixel detectors, *Microelectron. Eng.* 145 (2015) 133–137, <https://doi.org/10.1016/j.mee.2015.04.006>, 01679317.
- [6] A. Abada, et al., FCC-hh: the hadron collider: future circular collider conceptual design report volume 3, *Eur. Phys. J. Spec. Top.* 228 (4) (Jul. 2019) 755–1107, <https://doi.org/10.1140/epjst/e2019-900087-0>.
- [7] A. Abada, et al., FCC-ee: the Lepton collider, *Eur. Phys. J. Spec. Top.* 2019 2282 228 (2) (Jun. 2019) 261–623, <https://doi.org/10.1140/EPJST/E2019-900045-4>.
- [8] Y. Temiz, R.D. Lovchik, G.V. Kaigala, E. Delamarche, Lab-on-a-chip devices: how to close and plug the lab? *Microelectron. Eng.* 132 (Jan. 2015) 156–175, <https://doi.org/10.1016/j.mee.2014.10.013>.
- [9] P.K. Yuen, SmartBuild-A truly plug-n-play modular microfluidic system, *Lab Chip* 8 (8) (Jul. 2008) 1374, <https://doi.org/10.1039/b805086d>.
- [10] K. Vittayarukskul, A.P. Lee, A truly Lego®-like modular microfluidics platform, *J. Micromech. Microeng.* 27 (3) (Mar. 2017), 035004, <https://doi.org/10.1088/1361-6439/aa53ed>.
- [11] C.E. Owens, A.J. Hart, High-precision modular microfluidics by micromilling of interlocking injection-molded blocks, *Lab Chip* 18 (6) (Mar. 2018) 890–901, <https://doi.org/10.1039/C7LC00951H>.
- [12] C. Owens, Modular LEGO brick microfluidics, *Massachusetts Institute of Technology*, 2017. <https://dspace.mit.edu/handle/1721.1/117456>.
- [13] D.G. Johnson, R.D. Frisina, D.A. Borkholder, In-plane biocompatible microfluidic interconnects for implantable microsystems, *IEEE Trans. Biomed. Eng.* 58 (4) (Apr. 2011) 943–948, <https://doi.org/10.1109/TBME.2010.2098031>.
- [14] B. Dang, M.S. Bakir, J.D. Meindl, Integrated thermal-fluidic I/O interconnects for an on-chip microchannel heat sink, *IEEE Elect. Dev. Lett.* 27 (2) (Feb. 2006) 117–119, <https://doi.org/10.1109/LED.2005.862693>.
- [15] A. Francescon, et al., Development of interconnected silicon micro-evaporators for the on-detector electronics cooling of the future ITS detector in the ALICE experiment at LHC, *Appl. Therm. Eng.* (2015), <https://doi.org/10.1016/j.applthermaleng.2015.09.013>.
- [16] Accura® 25 PP Class [Online]. Available: <https://www.3dsystems.com/materials/accura-25-sla>, 2018.
- [17] M. Mager, ALPIDE, the Monolithic Active Pixel Sensor for the ALICE ITS upgrade, *Nucl. Inst. Methods Phys. Res. Sect. A Accel. Spectromet. Detect. Assoc. Equip.* 824 (Jul. 2016) 434–438, <https://doi.org/10.1016/j.nima.2015.09.057>.
- [18] M. Asadi, G. Xie, B. Sunden, A review of heat transfer and pressure drop characteristics of single and two-phase microchannels, *Int. J. Heat Mass Transf.* 79 (Dec. 2014) 34–53, <https://doi.org/10.1016/j.ijheatmasstransfer.2014.07.090>.
- [19] W. Rybiński, J. Mikieliewicz, Analytical solutions of heat transfer for laminar flow in rectangular channels, *Arch. Thermodyn.* 35 (4) (Jan. 2014) 29–42, <https://doi.org/10.2478/AOTER-2014-0031>.
- [20] Engineering Simulation | ANSYS. <https://www.ansys.com/>.
- [21] B. Abelev, et al., Technical design report for the upgrade of the ALICE inner tracking system, *J. Phys. G Nucl. Part. Phys.* 41 (8) (Aug. 2014) 087002, <https://doi.org/10.1088/0954-3899/41/8/087002>.
- [22] Ord 5700, Parker O-Ring Handbook [Online]. Available: <https://www.parker.com/Literature/O-RingDivision/Literature/ORD5700.pdf>, 2021.
- [23] How to Select, Design, and Install O-Ring Seals – Tarkka. <https://tarkka.co/2019/03/24/o-rings-o-yeah-how-to-select-design-and-install-o-ring-seals/>.
- [24] What is PolyJet Technology for 3D Printing? | Stratasys. <https://www.stratasys.com/polyjet-technology>.
- [25] Vero: A Realistic Multi-Color 3D Printing Material | Stratasys. <https://www.stratasys.com/materials/search/vero>.
- [26] T.J. Teo, A.H. Slocum, Principle of elastic averaging for rapid precision design, *Precis. Eng.* 49 (Jul. 2017) 146–159, <https://doi.org/10.1016/j.precisioneng.2017.02.003>.
- [27] D. Huo, K. Cheng, F. Wardle, *Design of Precision Machines*, in: K. Cheng (Ed.), *Machining Dynamics: Fundamentals, Applications and Practices*, Springer London, London, 2009, pp. 283–321.
- [28] Mitutoyo, “CRYSTA-APEX S SERIES.” [Online]. Available: [https://www.mitutoyo.com/wp-content/uploads/2013/01/2097\\_CRYSTA\\_ApexS.pdf](https://www.mitutoyo.com/wp-content/uploads/2013/01/2097_CRYSTA_ApexS.pdf).
- [29] U5100 High Accuracy Pressure Sensor [Online]. Available: <https://www.cdiweb.com/datasheets/te-us-5100.pdf>.